

## Effects of surfactant contamination on oxygen mass transfer in fine bubble aeration process

Xulu Chen, Guo-hua Liu, Haitao Fan, Meidi Li, Tao Luo, Lu Qi<sup>†</sup>, and Hongchen Wang<sup>†</sup>

School of Environment & Natural Resource, Renmin University of China, Beijing 100872, China  
(Received 23 November 2012 • accepted 21 May 2013)

**Abstract**—The effects of anionic, cationic, and non-ionic surfactants (SDS, SDBS, CTAB and Tween20) on oxygen mass transfer (OMT) in fine bubble aeration systems were investigated. The overall gas-liquid volumetric mass transfer coefficient ( $K_La$ ), specific interfacial area ( $a$ ), and liquid-side mass transfer coefficient ( $K_L$ ) parameters were used to assess the influence of the surfactants. At the same concentration, the different surfactants were observed to influence the  $K_La$  value as follows:  $K_La$  (SDBS) >  $K_La$  (SDS) >  $K_La$  (tween20) >  $K_La$  (CTAB). For all used surfactants, the overall trends showed a significant decrease in the  $K_La$  value at low concentrations (0-5 mg/L), while the  $K_La$  value recovered somewhat at high concentrations (10-20 mg/L). The decrease to the  $K_L$  value was found to be much larger than increase in the  $a$  value in the presence of surfactants. Furthermore, a simple model was established that provides an OMT prediction for different surfactants.

Key words: Surfactant, Fine-bubble Aeration, Mass Transfer, Interface Coverage Rate, OMT Prediction Model

### INTRODUCTION

Aeration is an important process for wastewater treatment that accounts for the largest fraction of energy costs, ranging from 45 to 75% of the operating cost [1-3]. Generally, interfacial gas transfer is created by either shearing the liquid surface with a mechanical aerator (mixer or turbine) or releasing air through spargers or porous materials [4]. Oxygen mass transfer (OMT) is the fundamental function of aeration, and improving the OMT efficiency can result in energy saving in the sewage treatment process. Submerged bubble aeration techniques are widely used in wastewater treatment plants and can be classified as coarse- and fine-bubble aeration based on the bubble size. In recent years, fine-bubble aeration has become increasingly popular in the sewage treatment field because of its superior OMT properties [5,6].

Because of their wide use in the petroleum, food, and pharmaceutical industries as emulsifiers and wetting agents, chemical and biological surfactants are one of most common contaminants in wastewater. The presence of these surfactants greatly influences OMT in the fine bubble aeration process. Interfacial accumulation of surfactants decreases mass transfer rates in aeration because of the increase in interfacial rigidity, and decreases the internal gas circulation and interfacial renewal rates [7-9]. Conversely, surfactants can improve the mass transfer coefficient by promoting smaller bubble production [10], and by improving the bubble surface viscosity and elasticity, which influences the gas bubble rise velocity and the gas hold-up [11,12].

OMT in fine aeration processes can be characterized by the overall gas-liquid volumetric oxygen mass transfer coefficient,  $K_La$ , where  $a$  is the gas-liquid interfacial area per unit volume of the liquid (specific interfacial area) and  $K_L$  is the liquid-side mass transfer coefficient.

Some researchers [13,14] have assessed the effects of surfactants on the liquid-side mass transfer coefficient ( $K_L$ ) using modeling and experimental methods.

In our previous studies [15], the  $K_La$  value was found to be related to the static interfacial tension and gas holdup in the sodium dodecyl sulfate (SDS) liquid phase. Our objective was to investigate the influence of different surfactant types (anionic, cationic, and non-ionic) on the  $K_La$  value in fine bubble aeration systems, and to study how they influence the mechanism by determining specific interfacial area and  $K_L$  values under controlled hydrodynamic conditions (e.g. air flow rate, temperature, etc.). In addition, an OMT-prediction model was established by measuring the adsorption characteristics of the surfactants at the gas-liquid interfaces.

### MATERIALS AND METHODS

#### 1. Materials

Surfactants are widely used for washing, food, cosmetics, and pharmaceutical industries. In China, anionic surfactants accounted for 70% of the total surfactant market volume, non-ionic surfactants were about 20%, and the others were about 10% [16].

The surfactants used in the present work included sodium dodecyl sulfate (SDS) [CAS NO:151-21-3], sodium dodecyl benzene sulfonate (SDBS) [CAS NO: 25155-30-0], dodecyltrimethylammonium bromide (CTAB) [CAS NO: 1119-94-4] and polyoxyethylene (20) (Tween-20) [CAS NO: 9005-64-5], which were supplied by Sigma-Aldrich (Sigma-Aldrich (Shanghai) Trading Co., Ltd., Shanghai) with a purity of 99% for all cases. The solutions were prepared by mass using a balance with a precision of  $\pm 10^{-7}$  kg, and tap water was used to prepare the liquid phases. Since the concentration of long-chain anionic surfactants (LAS) in China's municipal domestic wastewater is generally below 0-20 mg/L [17,18], the surfactant concentration used in our study ranged from 0 mg/L to 20 mg/L.

<sup>†</sup>To whom correspondence should be addressed.  
E-mail: whc@ruc.edu.cn, Qilu@ruc.edu.cn

**Table 1. Physical-chemical characteristics of surfactants**

Material	Formula	Type	$M_w$ (kg·kmol <sup>-1</sup> )	<sup>a</sup> HLB
SDS	C <sub>12</sub> H <sub>25</sub> SO <sub>4</sub> Na	Anionic	288.5	40
SDBS	C <sub>18</sub> H <sub>29</sub> SO <sub>3</sub> Na	Anionic	348.5	10.6
CTAB	C <sub>19</sub> H <sub>42</sub> BrN	Cationic	364.5	15.8
Tween-20	C <sub>58</sub> H <sub>114</sub> O <sub>26</sub>	Nonionic	1226	16.7

<sup>a</sup>HLB: Hydrophilic-lipophilic balance

The physical-chemical characteristics of the surfactants are listed in Table 1.

The hydrophilic-lipophilic balance (HLB), relates the hydrophilic and lipophilic characteristics of surfactants, and can be calculated by the empirical formula:

$$HLB = 7 + 11.71g \frac{M_w}{M_0} \quad (1)$$

where  $M_w$  and  $M_0$  are the molecular weights of the hydrophilic and lipophilic groups in the surfactant molecule structures, respectively.

## 2. Experimental Setup

As shown in Fig. 1, the experiments were conducted in an organic glass cube vessel (0.5 m×0.5 m×2.0 m). A fine-pore ceramic diffuser (Jiangsu Philip Environmental Protection Engineering Co., Ltd., Yixing) was installed on the bottom of the vessel, and was connected to a blower (WWA-0.4/7, Shanghai Rusin Industrial Co., Ltd., Shanghai). The airflow was monitored by a pressure gauge and regulated by a rotameter (Range: 0-2.5 m<sup>3</sup>/h). Fine bubbles were

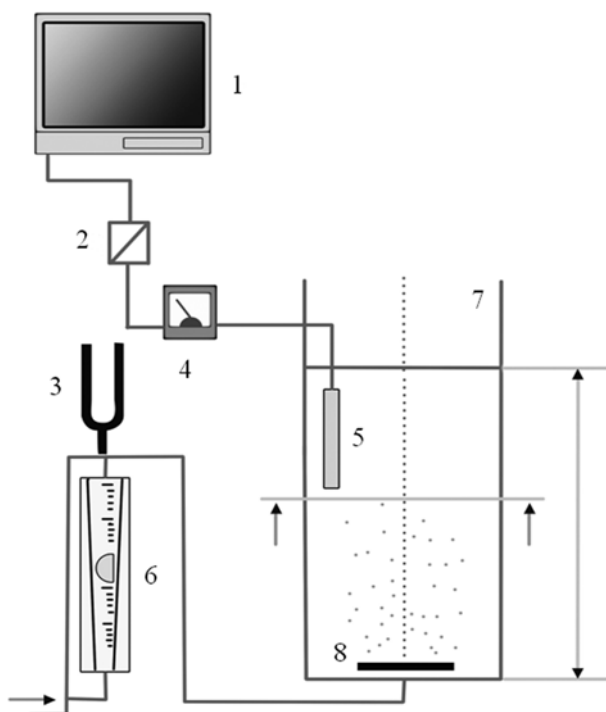


**Fig. 1. Schematic diagram of a fine bubble aeration system.**

- |                   |                     |
|-------------------|---------------------|
| 1. Data logger    | 5. DO probe         |
| 2. D/A converter  | 6. Rotameter        |
| 3. Pressure gauge | 7. Aeration tank    |
| 4. DO meter       | 8. Ceramic diffuser |

distributed through the bottom of the aeration vessel with the round ceramic diffuser at an airflow rate of 0.5 m<sup>3</sup>·h<sup>-1</sup>. A dissolved oxygen probe (LDO, Beijing Tianjian Innovative Instrument Co., Ltd., Beijing), with a 10-s response time, was used to monitor variations in the dissolved oxygen concentration in the center of the vessel. All chemical solutions were injected at the top of the vessel. The liquid height,  $H_L$ , was 1.5 m and the temperature was maintained at 293 K.

## 3. Methods

### 3-1. Specific Interfacial Area ( $a$ )

The specific interfacial area ( $a$ ) was determined according to the method reported by Painmanakul et al. [19]. In brief, the specific interfacial area is calculated as

$$a = N_B \times \frac{S_B}{V_{\text{total}}} = f_B \times \frac{H_L}{U_B} \times \frac{S_B}{AH_L + N_B V_B} \quad (2)$$

where  $A$  is the area of the aeration tank,  $H_L$  is the liquid height, and  $V_B$ ,  $r$ , and  $U_B$  are the bubble volume, bubble radius, and bubble velocity, respectively.  $f_B$  is the bubble formation frequency,  $N_B$  is the number of bubbles in the liquid phase, and  $S_B$  is the total bubble surface.

The parameters in Eq. (2) can be calculated according to the following formulas [19-21]:

$$v = \frac{2\pi R\gamma}{g\Delta\rho} \quad (3)$$

$$r = \left( \frac{3R\gamma}{2\Delta\rho g} \right)^{1/3} \quad (4)$$

$$U_B = \sqrt{2gr} \quad (5)$$

$$f_B = \frac{Q_G}{V_B} \quad (6)$$

$$N_B = f_B \times \frac{H_L}{U_B} \quad (7)$$

where  $R$  is the radius of the orifice,  $\gamma$  is the interfacial tension of liquid phase, and  $Q_G$  is the air flow rate.

### 3-2. Mass Transfer Coefficient

The  $K_L a$  value was determined by the two-film theory. It can be calculated as:

$$\frac{dc}{dt} = K_L a (C_S - C_t) \quad (8)$$

Integration of Eq. (8) gives:

$$\ln C_S - \ln (C_S - C_t) = K_L a \cdot t \quad (9)$$

Thus, the slope of a plot of the left-hand side of Eq. (9) versus time provides the  $K_L a$  value, where  $C_S$  is the dissolved oxygen saturation concentration and  $C_t$  is the measured instantaneous dissolved oxygen concentration at time  $t$ . The measured oxygen transfer rate in clean water has been reported by the American Society of Civil Engineers (ASCE, 2007) [22].

Total dissolved solids (TDS) were measured each time, and the value was approximately 300-400 mg/L. The  $K_L a$  was calculated after normalizing TDS concentration value (1,000 mg/L) based on the ASCE. All experiments were repeated three times in our study, and the relative standard deviation of all values used was less than

10%.

The product of  $K_L$  and  $a$  values is known as the  $K_L a$ . Thus, the  $K_L a$  value can be simply determined by

$$K_L a = \frac{K_L a}{a} \quad (10)$$

### 3-3. Liquid-phase Characterization

The examined liquid phases included tap water and aqueous solutions with four different surfactants (anionic, cationic, and non-ionic types). Their density and viscosity are all  $997 \text{ kg/m}^3$  and  $10^3 \text{ Pa}\cdot\text{s}$ , respectively.

The static interfacial tension of the solutions was measured by the DuNouy ring method with an interfacial tension apparatus (Sigma 703D, KSV NIMA, Helsinki). The kinetics of adsorption and diffusion of the surfactant molecules can be described according to the following equations based on Langmuir theory [23]:

$$Se = \frac{\Gamma_e}{\Gamma_\infty} = \frac{KC}{1+KC} \quad (11)$$

$$\gamma_0 - \gamma_e \approx RT\Gamma_\infty \text{Log}(K) + RT\Gamma_\infty \text{Log}(C) \quad (12)$$

where  $Se$  is the equilibrium surface coverage ratio,  $C$  is the solute concentration,  $\Gamma_\infty$  is the saturated adsorption capacity,  $K$  is the adsorption constant at equilibrium,  $\gamma_0$  and  $\gamma_e$  are the interfacial tension of tap water and a certain solution, respectively, and  $T$  is the adsorption temperature (293 K).

## RESULTS AND DISCUSSION

To make the  $K_L a$  value closer to the actual operating conditions in sewage treatment plant, the air flow rate and the orifice radius in the present were designed with  $0.5 \text{ m}^3/\text{h}$  and  $250 \mu\text{m}$ , respectively.

### 1. Effect of Surfactants on the Specific Interfacial Area ( $a$ )

The density and viscosity of the four surfactant solutions over the 0-20 mg/L concentration range were measured as  $0.997 \text{ g/cm}^3$  and  $1.01 \times 10^{-3} \text{ Pa}\cdot\text{s}$ , respectively, which are close to those in tap water. The static interfacial tensions of the surfactant solutions used in the fine bubble aeration process are presented in Table 2.

According to Eqs. (2)-(7), the specific interfacial area for the different surfactant solutions was calculated, and the relationship between the specific interfacial area and solution concentration for the different surfactants is shown in Fig. 2. In Fig. 2, the specific interfacial area values in each surfactant solution were found to be larger than those in clean water, and increased with increasing surfactant concentration. Hence, increasing the surfactant concentration has a positive effect on the OMT, which is in agreement with

**Table 2. Static surface tension of liquid phase**

C (mg/L)	SDS	SDBS	CTAB	Tween 20
0	72.66	72.66	72.66	72.66
1	70.60	58.50	67.28	64.50
3	64.54	48.98	62.38	60.39
5	60.11	40.74	59.03	55.73
10	51.11	35.07	54.98	51.94
15	46.99	32.64	52.14	48.28
20	47.06	30.88	50.27	46.87

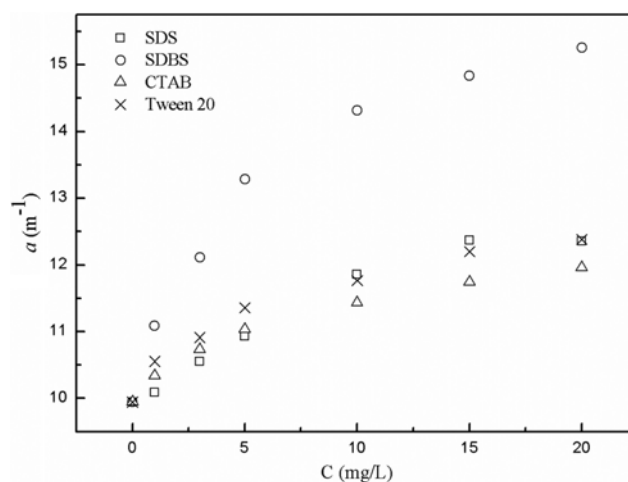


**Fig. 2. Specific interfacial area versus concentrations for several surfactants.**

the results reported by Painmanakul et al. [13]. For the same concentrations, the specific interfacial area values in different surfactant solutions were observed to be different, and indicated a varying trend as the surfactant concentration ranged from 0 to 20 mg/L:

0-5 mg/L:  $a(\text{SDBS}) > a(\text{Tween 20}) > a(\text{CTAB}) > a(\text{SDS})$ ;

10-20 mg/L:  $a(\text{SDBS}) > a(\text{SDS}) > a(\text{Tween 20}) > a(\text{CTAB})$ .

As shown in Fig. 2, the  $a$  in SDBS solutions was found to be much larger than that in other surfactants under any concentration. This may be because the HLB value of the SDBS is higher than that of the other surfactants (Table 1), indicating stronger hydrophilic property and weaker adsorption ability on gas-liquid interface for SDBS.

### 2. Effect of Surfactants on OMT Coefficients

The effect of surfactant type and concentration on the OMT coefficients containing  $K_L a$  and  $K_L$  was assessed.

#### 2-1. Effect of Surfactants on $K_L a$

As shown in Fig. 3, an increase in the surfactant concentration leads to a sharp decrease in  $K_L a$ , especially in the surfactant concentration range of 0-5 mg/L. The trend in the  $K_L a$  decrease became

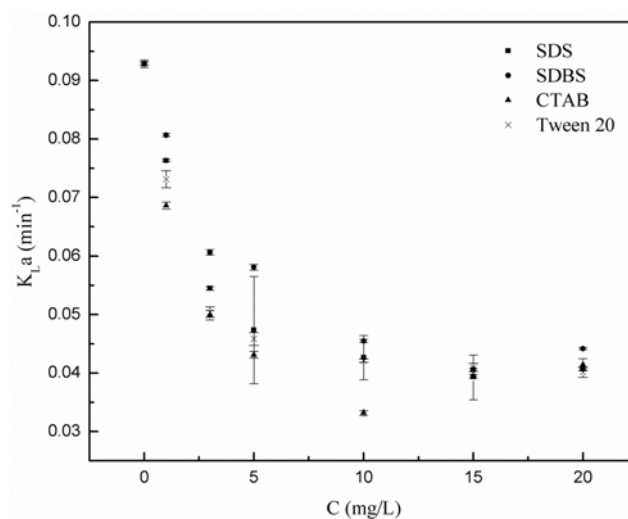


**Fig. 3. Effects of surfactant type and concentration on  $K_L a$ .**

gentle when the surfactant concentration was increased up to 5 mg/L, and the smallest  $K_L a$  value for all the surfactants used occurred in the concentration range of 10-15 mg/L. Although the  $K_L a$  values began to recover at high surfactant concentration (>15 mg/L), they were still lower than that ( $0.033 \text{ min}^{-1}$ ) in clean water. These results suggested that the surfactants, even small amounts, could have a significant effect on the OMT in the fine bubble aeration process. Our results were observed to be similar to results reported by Eckenfelder and Barnhart [24], who found that the  $K_L a$  value decreases with increasing sodium lauryl sulfate concentrations (0-75 mg/L). The  $K_L a$  value reached a minimum at low surfactant concentrations, and partially recovered at higher concentrations.

At the same concentrations, the different surfactants were observed to influence the  $K_L a$  value as follows:  $K_L a$  (SDBS) >  $K_L a$  (SDS) >  $K_L a$  (tween20) >  $K_L a$  (CTAB), that is,  $K_L a$  (anionic) >  $K_L a$  (nonionic) >  $K_L a$  (cationic). The trend was more obvious at surfactant concentrations below 10 mg/L. The two anionic surfactants (SDS and SDBS) displayed different effects on the OMT, with the low-molecular-weight SDS having a more notable inhibition effect than SDBS. This may be due to differences in their structures and properties [25]. Rosso and Stenstrom [26] used molecular weight to explain this phenomenon, suggesting that as time elapses, the  $K_L a$  decreases rapidly because the low-molecule-weight surfactant migrates faster towards the bubble surface.

2-2. Effect of Surfactants on  $K_L$

Fig. 4 shows the  $K_L$  values obtained with a range of surfactant concentrations for different surfactants. The concentration-dependent  $K_L$  value trends were found to be similar in the presence of different surfactants. The  $K_L$  value decreased substantially with only a slight increase in the surfactant concentration. The relative ordering of  $K_L$  values for different surfactants over the 0 to 5 mg/L concentration range was observed to be:

$$K_L (\text{SDS}) > K_L (\text{SDBS}) > K_L (\text{Tween 20}) > K_L (\text{CTAB})$$

As the surfactant concentration was further increased up to 10 mg/L, the effects of surfactants on  $K_L$  were essentially independent. This may be because surfactant concentration at the interface remains unchanged at higher concentrations.

However, the  $K_L a$  relationship for the two anionic surfactants (SDS

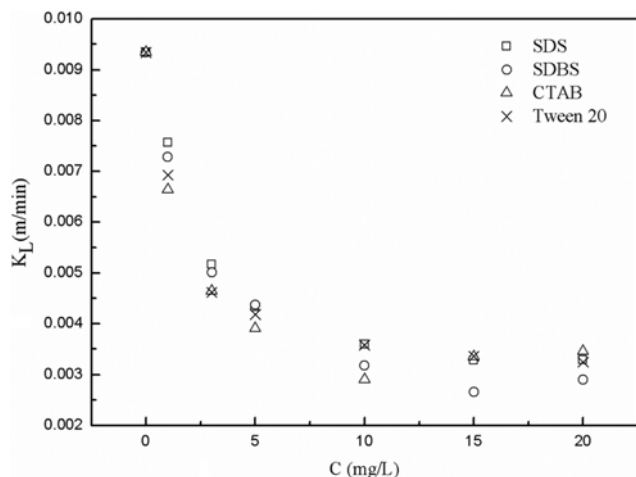


Fig. 4. Effects of different surfactants on the  $K_L$  value.

and SDBS) was found to be contrary (see the results explained above). This behavior can be rationalized because the specific interfacial area in the SDBS solution is much larger than that in SDS solution (see Fig. 2), and thus the positive influence of the specific interfacial area offsets the adverse influence of the low  $K_L$  on the overall  $K_L a$  value.

3. Relationship between Interface Coverage Rate and  $K_L$  for Different Surfactants

To explain the surfactant effect on  $K_L$ , the surface coverage ratio (Se) (derived from interfacial tension measurements) was used to assess the liquid-phase adsorption characteristics of different surfactant solutions. The Se is introduced to imply the “area” left unoccupied on the surface that oxygen molecules may pass through,  $Se = (I/I_\infty)$ . Se values between 0 and 1 imply that the interface is partially occupied by surfactant molecules under the saturation concentration [14]. In previous studies the  $K_L$  value has been shown to be related to the dynamic interfacial tension [27-29]. However, the relationship between  $K_L$  and static interfacial tension ( $\gamma$ ) has not been established. Since the  $K_L$  value was equal to the  $a$  value under adsorption equilibrium conditions in our study, the static interfacial tension is suitable for explaining the influence of different surfactants on  $K_L$ . Fig. 5 shows the relationship between Se and surfactant concentration, indicating that Se increased rapidly with increasing concentration over the 0-10 mg/L range, and increased little when the surfactant concentration was further increased up to 20 mg/L. This may be because most of the adsorption process has occurred at low concentrations. In the concentration range 1-5 mg/L, the Se trend for different surfactants can be found as follows:

$$Se (\text{SDBS}) > Se (\text{Tween 20}) > Se (\text{CTAB}) > Se (\text{SDS}).$$

Although similar relationships have been reported before, an explanation for this behavior has not been presented. Taking into account the presence of active surface substances in gas-liquid interfaces, a new model [14] has been developed for different bubble size generated under different air flow rates. The bubble size range is divided into three zones: zone A ( $d_b < 1.5 \text{ mm}$ ), zone B ( $1.5 \text{ mm} < d_b < 3.5 \text{ mm}$ ) and zone C ( $d_b > 3.5 \text{ mm}$ ). This model predicts, under the experimental conditions employed in their works, that the mass transfer coefficient must be included between two limits:  $k_L^0$ , mass transfer

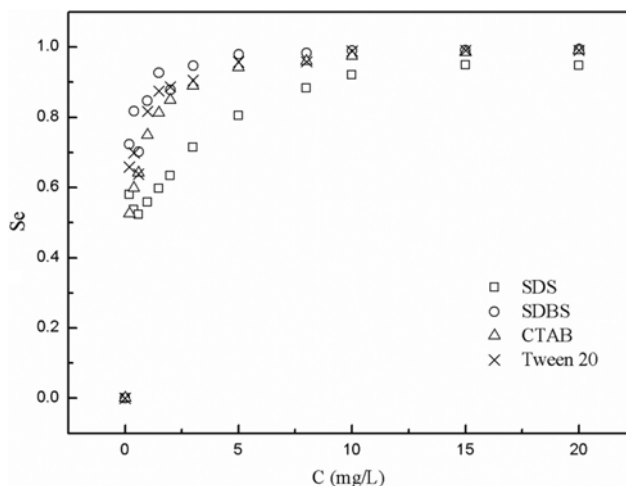


Fig. 5. Interfacial coverage for different solutions.

coefficient for free surface ( $Se=0$ ) and  $k_L^1$ , mass transfer coefficient for a saturated surface ( $Se=1$ ).

García-Abuín [30] found the model did not fit the prediction of the mass transfer coefficient at a low concentration of the surfactants with small chain length. In our study, this model was also found not to be suitable for the surfactant solution with low concentrations.

The  $Se$  value was observed to be closely related to the HLB values of the surfactants. That is, for different surfactants, the lower the HLB value, the higher the  $Se$  value. This trend may be understood as a result of the molecular mass ratio of lipophilic groups in the surfactant molecule influencing surfactant migration. Generally, the molecule accumulates easily at the gas-liquid interface for surfactants with a higher ratio and leads to a higher  $Se$  value.

The  $Se$  for surfactant solutions has a strong negative effect on  $K_L$ , and this effect is larger than the positive effect of the specific area. Therefore, it is important to understand the relationship between  $Se$  and  $K_L$  to determine the effect of surfactants on OMT. To facilitate the comparison of  $K_L$  values in different surfactant solutions, a dimensionless parameter ( $\eta$ ) was introduced to represent OMT inhibition. The OMT inhibition rate is taken to be  $\eta=K_L/K_L^0$ , where  $K_L$  and  $K_L^0$  are the liquid-side mass transfer coefficients in surfactant solution and tap water, respectively. On the basis of our measured  $K_L$  and  $Se$  values for the different surfactants, the relationship between  $\eta$  and  $Se$  was determined to obey the following fit equations:

$$\eta = 1.23 - 0.22e^{\frac{Se}{0.67}} \quad (13)$$

$$\eta = 1.00 - 0.0009e^{\frac{Se}{0.15}} \quad (14)$$

$$\eta = 1.07 - 0.065e^{\frac{Se}{0.4}} \quad (15)$$

$$\eta = 1.04 - 0.037e^{\frac{Se}{0.33}} \quad (16)$$

Most of the measured data agreed with the above equations within  $\pm 10\%$  of an exact agreement, as shown in Fig. 6.

Based on the equations above, the relationship between  $\eta$  and  $Se$  for a given surfactant can be expressed as the following formula:

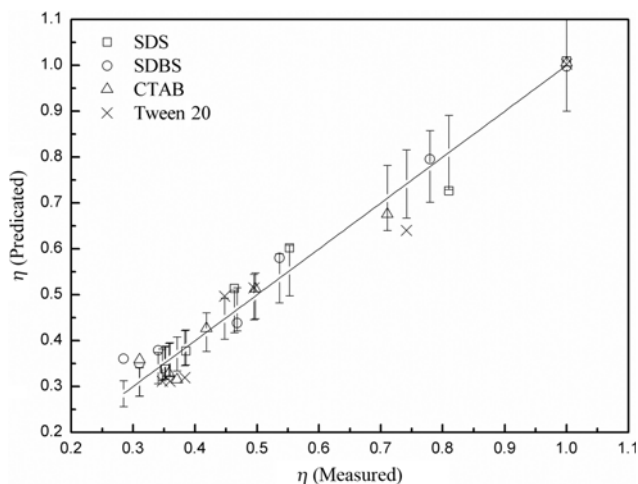


Fig. 6. Predicted  $K_L$  (Eqs. (13)-(16)) versus measured data.

$$\eta = b - ke^{\frac{Se}{t}} \quad (17)$$

where  $b$ ,  $k$ , and  $t$  are empirical constants.  $b=k+1$  and  $t$  is a constant which shows a positive correlation with the HLB value. The ratio of  $t/HLB$  is 0.15 to 0.25.

Although two models to predict  $K_L$  have been proposed by Higbie [31] and Frossling [32], their application is limited to the two extreme conditions of clean, large bubbles and dirty, small bubbles. Furthermore, a model relating  $K_L$  and  $Se$  has also been established by Painmanakul et al. [19] based on the previous two extreme models. The Painmanakul model presents this relation as  $K_L = S_e K_L^1 + (1 - S_e) K_L^0$ , where  $K_L^1$  and  $K_L^0$  are the liquid-side mass transfer coefficients for free and saturated surfaces, respectively. Sardeing et al. [14] developed this model further by applying it to assess different bubble sizes generated under different air flow rates. In our study, these established models failed to fit the mass transfer coefficient values at low surfactant concentrations, which is in agreement with other results reported by García-Abuín [30]. As an alternative predictive tool, our model offers a simple method to predict the OMT inhibition rate for different surfactants.

## CONCLUSIONS

Surfactants have a strong inhibition effect on  $K_L a$ , which is a comprehensive result based on influences of the surfactants on  $K_L$  and the specific interfacial area. Since the negative effect of surfactants on  $K_L$  values is more notable than the positive effect on the specific interfacial area, the  $K_L a$  value tended to decrease significantly at low concentrations (0-5 mg/L), while recovering somewhat at high concentrations (10-20 mg/L). At the same concentration, the different surfactants were observed to influence  $K_L a$  as follows:  $K_L a$  (SDBS)  $> K_L a$  (SDS)  $> K_L a$  (Tween20)  $> K_L a$  (CTAB). The effect of surfactants on  $K_L$  was closely related to the  $Se$ . Based on our experimental data, a relationship between  $K_L$  and  $Se$  can be given as  $\eta = b - ke^{\frac{Se}{t}}$ , where  $\eta$  is the ratio of the  $K_L$  values for the free and saturated surfaces;  $b$ ,  $k$ , and  $t$  are empirical constants;  $b=k+1$ ; and  $t$  shows a positive correlation with HLB value (the ratio  $t/HLB$  is 0.15 to 0.25). The simple model allows prediction of the OMT inhibition rate for different surfactants.

## NOTATION

- $a$  : specific interfacial area [ $m^{-1}$ ]
- $A$  : area of aeration tank [ $m^2$ ]
- $C$  : surfactant solution concentration [ $mg/L$ ]
- $C_S$  : saturation concentration of dissolved oxygen [ $mg/L$ ]
- $C_t$  : measured instantaneous concentration of dissolved oxygen at time  $t$  [ $mg/L$ ]
- $f_B$  : bubble formation frequency [ $s^{-1}$ ]
- $H_L$  : liquid height [ $m$ ]
- HLB : hydrophilic-lipophilic balance, dimensionless
- $K$  : adsorption constant at equilibrium [ $m^3/mol$ ]
- $K_L$  : liquid-side mass transfer coefficient [ $m/min$ ]
- $K_L a$  : overall gas-liquid volumetric mass transfer coefficient [ $min^{-1}$ ]
- $M_0$  : molecular weight of lipophilic groups [ $kg/kmol$ ]
- $M_w$  : molecular weight of hydrophilic groups [ $kg/kmol$ ]

$N_B$  : number of bubbles in liquid phase, dimensionless  
 OMT : oxygen mass transfer  
 $Q_G$  : air flow rate [ $\text{m}^3/\text{h}$ ]  
 $R$  : the radius of the orifice [m]  
 $S_B$  : total bubble surface [ $\text{m}^2$ ]  
 $Se$  : surface coverage ratio at equilibrium, dimensionless  
 $T$  : temperature [K]  
 $U_B$  : bubble velocity [m/s]  
 $V_B$  : bubble volume [ $\text{m}^3$ ]  
 $r$  : bubble radius [m]

### Greek Letters

$\gamma$  : static interfacial tension [ $\text{mN/m}$ ]  
 $\gamma_0$  : interfacial tension of tap water and a certain solution [ $\text{mN/m}$ ]  
 $\gamma_e$  : surface tension of a certain solution [ $\text{mN/m}$ ]  
 $\eta$  : OMT inhibition rate, dimensionless  
 $\Gamma_e$  : adsorption capacity [ $\text{mol/m}^2$ ]  
 $\Gamma_\infty$  : saturated adsorption capacity [ $\text{mol/m}^2$ ]

### ACKNOWLEDGEMENT

This work was supported by the National High-tech R&D Program (no. 2009AA063804) and the National Science and Technology Major Project - Water Pollution Control and Management of china (no. 2011ZX07316-001).

### REFERENCES

1. R. G. Rice and S. W. Howell, *AIChE J.*, **32**, 1377 (1986).
2. D. J. Reardon, *Civ. Eng.*, **65**, 54 (1995).
3. Y. Fayollea, A. Cockxb, S. Gillota, M. Roustan and A. Héduit, *Chem. Eng. J.*, **62**, 7163 (2007).
4. P. Painmanakul and G. Hébrard, *Chem. Eng. Res. Des.*, **86**, 1207 (2008).
5. V. L. Burris and J. C. Little, *Water Sci. Technol.*, **37**, 293 (1988).
6. D. F. McGinnis and J. C. Little, *Water Res.*, **36**, 4627 (2002).
7. D. Rosso, Ph.D thesis, University of California Los Angeles (2005).
8. D. Rosso, D. L. Huo and M. K. Stenstrom, *Chem. Eng. Sci.*, **66**, 5500 (2006a).
9. D. Rosso, D. L. Huo and M. K. *Water Res.*, **40**, 1397 (2006b).
10. J. M. Chern, S. R. Chou and C. H. Shang, *Water Res.*, **35**, 3041 (2001).
11. A. Tzounakos, D. G. Karamanev, A. Margaritis and M. A. Bergougnou, *Ind. Eng. Chem. Res.*, **43**, 5790 (2004).
12. S. S. Alves, S. P. Orvalho and J. M. T. Vasconcelos, *Chem. Eng. Sci.*, **60**, 1 (2005).
13. P. Painmanakul, K. Loubière, G. Hébrard, M. Mietton-Peuchot and M. Roustan, *Chem. Eng. Sci.*, **60**, 6480 (2005).
14. R. Sardeing, P. Painmanakul and G. Hébrard, *Chem. Eng. Sci.*, **61**, 6249 (2006).
15. X. L. Chen, H. C. Wang, L. Qi, T. Luo, H. T. Fan and M. D. Li, *Acta Sci. Circum.*, **33**, 2 (2013).
16. A. X. Jiang, B. Xia and Y. X. Li, *Safety and Environ. J.*, **4**, 2 (2004).
17. H. C. Wang, *Municipal Eng. Tech.*, **1**, 30 (1997).
18. L. P. Liu, *Environ. Sci. Survey*, **29**, 1 (2010).
19. P. Painmanakul, K. Loubière, G. Hébrard and P. Buffière, *Chem. Eng. Proc.*, **43**, 1347 (2004).
20. <http://www.seas.ucla.edu/stenstro/Bubble.pdf>.
21. S. J. Zhang, *Research on the three-dimensional numerical simulation of bubble dynamics*, Hohai University (2006).
22. ASCE, American Society of Civil Engineers-ASCE/EWRI 2-06, New York (2007).
23. K. Loubière and G. Hébrard, *Chem. Eng. Proc.*, **43**, 1361 (2004).
24. W. W. Eckenfelder and E. L. Barnhart, *AIChE J.*, **17**, 631 (1961).
25. C. Liu, L. Zhang, J. L. Yang, J. B. Guo and Z. X. Li, *Energy Environ. Tech.*, **2**, 531 (2009).
26. D. Rosso and K. M. Stenstrom, *Water Environ. Res. Foundation*, **6**, 4853 (2006).
27. M. K. Stenstrom and R. G. Gilbert, *Water Res.*, **15**, 643 (1981).
28. M. Wagner and R. J. Popel, *Water Sci. Technol.*, **34**, 249 (1996).
29. T. L. Huo, Ph.D thesis, University of California (1998).
30. A. García-Abuín, D. Gómez-Díaz, J. M. Navaza and B. Sanjurjo, *Chem. Eng. Sci.*, **65**, 4484 (2010).
31. R. Higbie, *Trans. Am. Inst. Chem. Eng.*, **31**, 365 (1935).
32. N. Frössling, *Gerlands Beitr. Geophys.*, **52**, 170 (1938).